Bull. Mater. Sci., Vol. 39, No. 7, December 2016, pp. 1665–1670. © Indian Academy of Sciences.
DOI 10.1007/s12034-016-1330-8

Effects of Zn doping concentration on resistive switching characteristics in $Ag/La_{1-x}Zn_xMnO_3/p^+$-Si devices

SHUAISHUAI YAN[1,2], HUA WANG[1,2,*], JIWEN XU[1,2], LING YANG[1,2], WEI QIU[1,2], QISONG CHEN[1,2] and DONG HAN[1,2]

[1]School of Materials Science and Engineering, Guilin University of Electronic Technology, Guilin 541004, People's Republic of China

[2]Guangxi Key Laboratory of Information Materials, Guilin University of Electronic Technology, Guilin 541004, People's Republic of China

MS received 19 May 2015; accepted 6 May 2016

Abstract. **$Ag/La_{1-x}Zn_xMnO_3/p^+$-Si devices with different Zn doping contents were fabricated through sol–gel method. The effects of Zn doping concentration on the microstructure of $La_{1-x}Zn_xMnO_3$ films, as well as on the resistance switching behaviour and endurance characteristics of $Ag/La_{1-x}Zn_xMnO_3/p^+$-Si were investigated. After annealing at 600°C for 1 h, the $La_{1-x}Zn_xMnO_3$ ($x = 0.1, 0.2, 0.3, 0.4, 0.5$) are amorphous and have bipolar resistance characteristics, with R_{HRS}/R_{LRS} ratios $>10^3$. However, the endurance characteristics show considerable differences; $x = 0.3$ shows the best endurance characteristics in more than 1000 switching cycles. The conduction mechanism of the $Ag/La_{1-x}Zn_xMnO_3/p^+$-Si is the Schottky emission mode at high resistance state. However, the conduction mechanism at low resistance state varies with Zn doping concentration. The dominant mechanism at $x = 0.1$ is filamentary conduction mechanism, whereas that at $x \geq 0.2$ is space-charge-limited current conduction.**

Keywords. **$La_{1-x}Zn_xMnO_3$; amorphous; resistance switching; sol–gel.**

1. Introduction

Resistive random access memory (RRAM) with a small size, high storage density, low operation voltage and high reading speed has attracted considerable research interest [1,2]. A RRAM cell is generally composed of an insulator sandwiched between two electrons (M-I-M), which can be electrically switched between high resistance state (HRS) and low resistance state (LRS). Up to the present, resistive switching (RS) properties have been observed in many materials, such as perovskite oxides [3,4], binary metal oxides [5,6], solid-state electrolytes [7] and organic compounds [8]. The perovskite $Re_{1-x}A_xMnO_3$ (Re = Pr, La, A = Ca, Sr) [9–11] has been given particular attention because of its potential applications in high-performance non-volatile RRAM devices; however, most reports focused on crystallinity, and no other doped element was reported. The annealing temperature of amorphous films is lower than that of crystalline films, which are more compatible with CMOS technology. Although the switching behaviour has been studied for decades, the switching mechanisms remain unclear.

This study aims to investigate the effects of Zn doping concentration on the microstructure of $La_{1-x}Zn_xMnO_3$ films, as well as on the resistance switching behaviour and endurance characteristics of $Ag/La_{1-x}Zn_xMnO_3/p^+$-Si devices.

2. Experimental

The $La_{1-x}Zn_xMnO_3$ ($x = 0.1, 0.2, 0.3, 0.4, 0.5$) thin films were prepared on p^+-Si substrates by sol–gel spin coating technique using $Mn(CH_3COO)_2{\cdot}4H_2O$, $Zn(CH_3COO)_2{\cdot}2H_2O$ and $La(NO_3)_3{\cdot}6H_2O$ powders as the sources, 2-methoxyethanol as solvent and diethanolamine as stabilizer. Thin films were prepared by spin coating the homogeneous solution at 4000 rpm for 30 s, followed by preheating at 120°C for 5 min and then at 400°C for 15 min. The above process was repeated for four times. The films were approximately 210 nm thick. Finally, the thin films were annealed at 600°C for 1 h in ambient air. The top Ag electrodes were deposited through vacuum evaporation method with a metal shadow mask forming a structure of $Ag/La_{1-x}Zn_xMnO_3/p^+$-Si.

The phases of films were characterized by X-ray diffraction (XRD, AXS D8-ADVANCE, Bruker). The surface morphologies and thickness of $La_{1-x}Zn_xMnO_3$ films were observed through scanning electron microscope (SEM, Hitachi S4800). The current–voltage (I–V) curves of the $Ag/La_{1-x}Zn_xMnO_3/p^+$-Si devices were obtained using Keithley 2400 source meter at room temperature.

3. Results and discussion

Figure 1 shows the XRD patterns of the $La_{1-x}Zn_xMnO_3/p^+$-Si ($x = 0.1, 0.2, 0.3, 0.4, 0.5$) heterojunction and p^+-Si. Except for the diffraction peaks of p^+-Si, the diffraction

*Author for correspondence (wh65@tom.com)

peaks of $La_{1-x}Zn_xMnO_3$ were undetected, which indicated that the $La_{1-x}Zn_xMnO_3$ films grown on the p^+-Si (100) substrate were amorphous after annealing at 600°C for 1 h in ambient air. The surfaces of the $La_{1-x}Zn_xMnO_3$ films were characterized by SEM (figure 2a–e). The images reveal the granular microstructure because of the volatilization of organic matter by sol–gel technology. The almost uniform roughness was a result of small variations in the Zn doping concentration. The cross-section of the films is presented in figure 2f. Only one specimen with $x = 0.3$ is shown because their cross-sections are similar, where a clear interface between $La_{1-x}Zn_xMnO_3$ and substrate p^+-Si can be observed, without any evidence of interfacial reactions. The thickness of the $La_{1-x}Zn_xMnO_3$ films is approximately 215 nm, as shown in figure 2f.

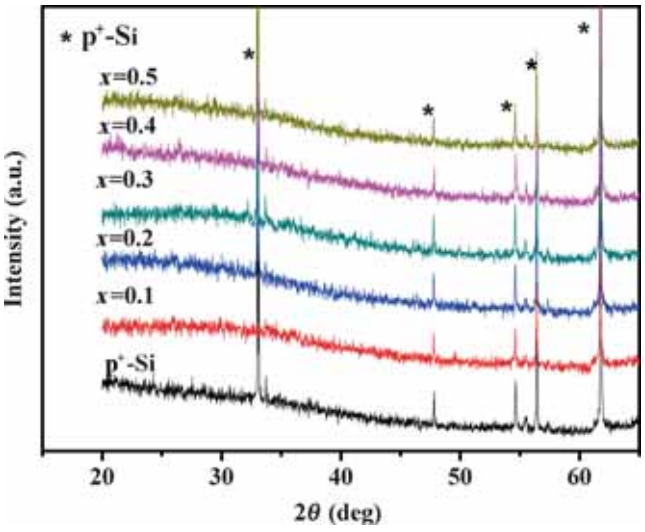

Figure 1. XRD patterns of the $La_{1-x}Zn_xMnO_3/p^+$-Si heterojunction and the p^+-Si.

Figure 3 shows the typical I–V characteristics of $Ag/La_{1-x}Zn_xMnO_3/p^+$-Si devices in semi-logarithmic scales, which reveal the typical bipolar resistance switching behaviour. The voltage bias was swept in a sequence of $0 \rightarrow 6 \rightarrow -6 \rightarrow 0$ V at room temperature. By steadily increasing the positive voltage imposed on the $Ag/La_{1-x}Zn_xMnO_3/p^+$-Si device, resistance of the devices suddenly decreased from HRS to LRS at approximately 4 V (set voltage), which is called 'set' progress. Subsequently, when sweeping the voltage in reverse to negative values, the 'reset' progress could be seen, as evidenced by the resistance switching from LRS

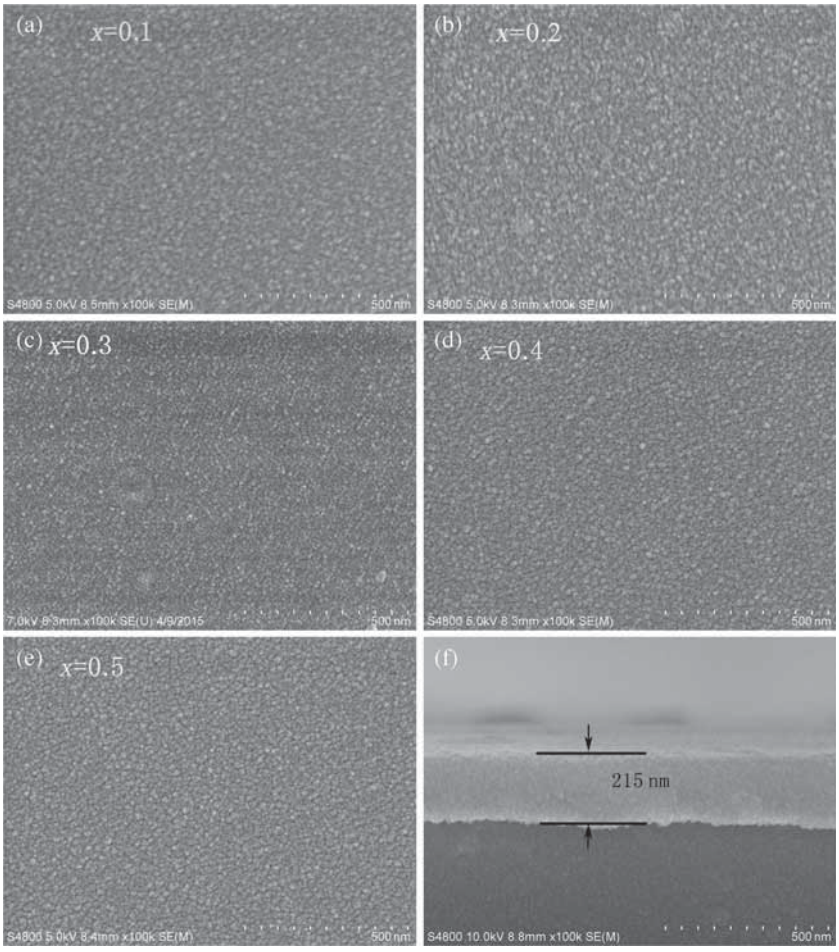

Figure 2. SEM images of (**a–e**) surface and (**f**) cross-section morphology of the $La_{1-x}Zn_xMnO_3/p^+$-Si.

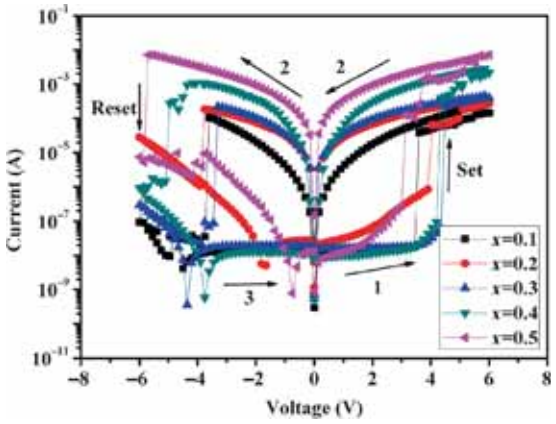

Figure 3. I–V curves of the $Ag/La_{1-x}Zn_xMnO_3/p^+$-Si devices in semi-logarithmic scales.

to HRS again at reset voltage. Different Zn doping concentrations correspond to different reset voltages. At $x = 0.1$, 0.2, 0.3, 0.4, the reset voltages are approximately -4 V; however, the reset voltage is -6 V at $x = 0.5$. The defect density may change with the increase of the amount of doped Zn because of $R_{Zn}^{2+} < R_{La}^{3+}$ [12], accounting for the difference of the reset voltages. When the bias voltage sweeps from -6 to 0 V, the current reached the minimum value at a certain voltage, which indicated the hysteresis of the capacitance of the devices.

To clarify the conduction and switching mechanisms of the devices, the I–V characteristics are replotted in the ln–ln scale. As shown in figure 4, for the HRS the slope of the I–V characteristic is smaller than 1 at low electric fields. In addition, the current is mainly caused by the intrinsic carrier and small amounts of injected carrier under a low electric

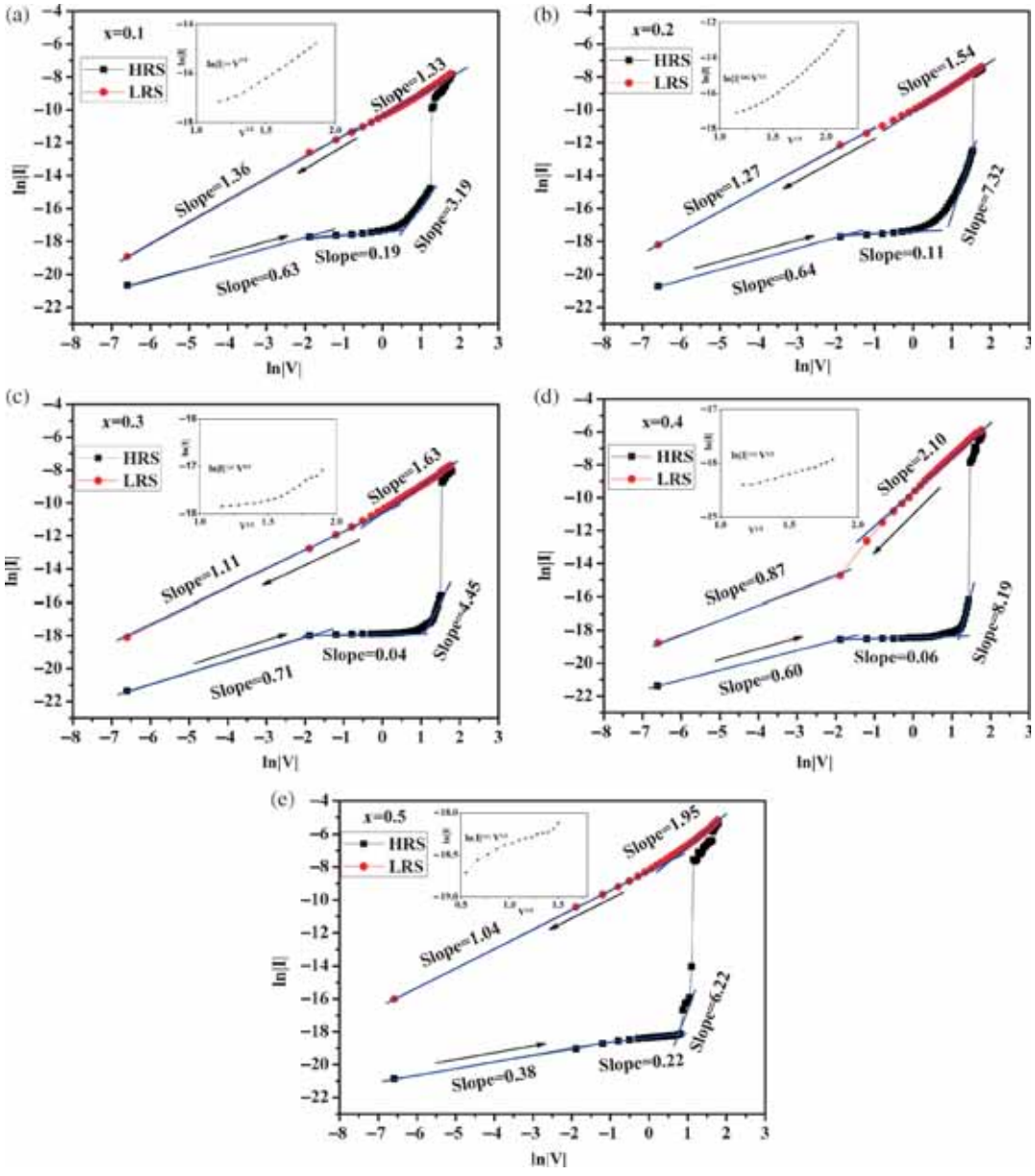

Figure 4. Linear fitting for the I–V curve of the $Ag/La_{1-x}Zn_xMnO_3/p^+$-Si in ln–ln scale and corresponding slops for each portion.

field. The slope is much lower and then gradually increases with the increase in voltage. The conduction follows the behaviour of the Schottky emission mode [13] because of the Schottky barrier formed in the interface between LZMO and Ag at low electric fields, as evidenced by the curve showing a line in the $\ln|I| \propto V^{1/2}$ in the inset of figure 4. The slopes are different when the resistance switches from HRS to LRS. At high electric fields, as can be seen in figure 4a, the slope is 1.33, close to 1; however, as shown in figures 4b–e, the slope is approximately 2. The slopes then all gradually decreased to approximately 1. The Schottky barrier changes with the change in voltage bias. Then, the dominant conduction mechanism gradually changes from Schottky emission to filamentary or space-charge-limited current (SCLC). The curve at $x = 0.1$ can be explained by filamentary mode [14–16], which is formed by oxygen vacancy or electrode Ag^+, and the RS of LZMO is a displacement of oxygen vacancies located at the bottom of Ag/LZMO interface. The curve at $x \geq 0.2$ can be explained by SCLC [17–20]. As an inevitable defect, oxygen vacancies exist in the $La_{1-x}Zn_xMnO_3$ thin films, these vacancies act as trap centres for charge carriers leading to the trap-controlled SCLC transport behaviour. With the increase in Zn doping concentration, the trapping of defects

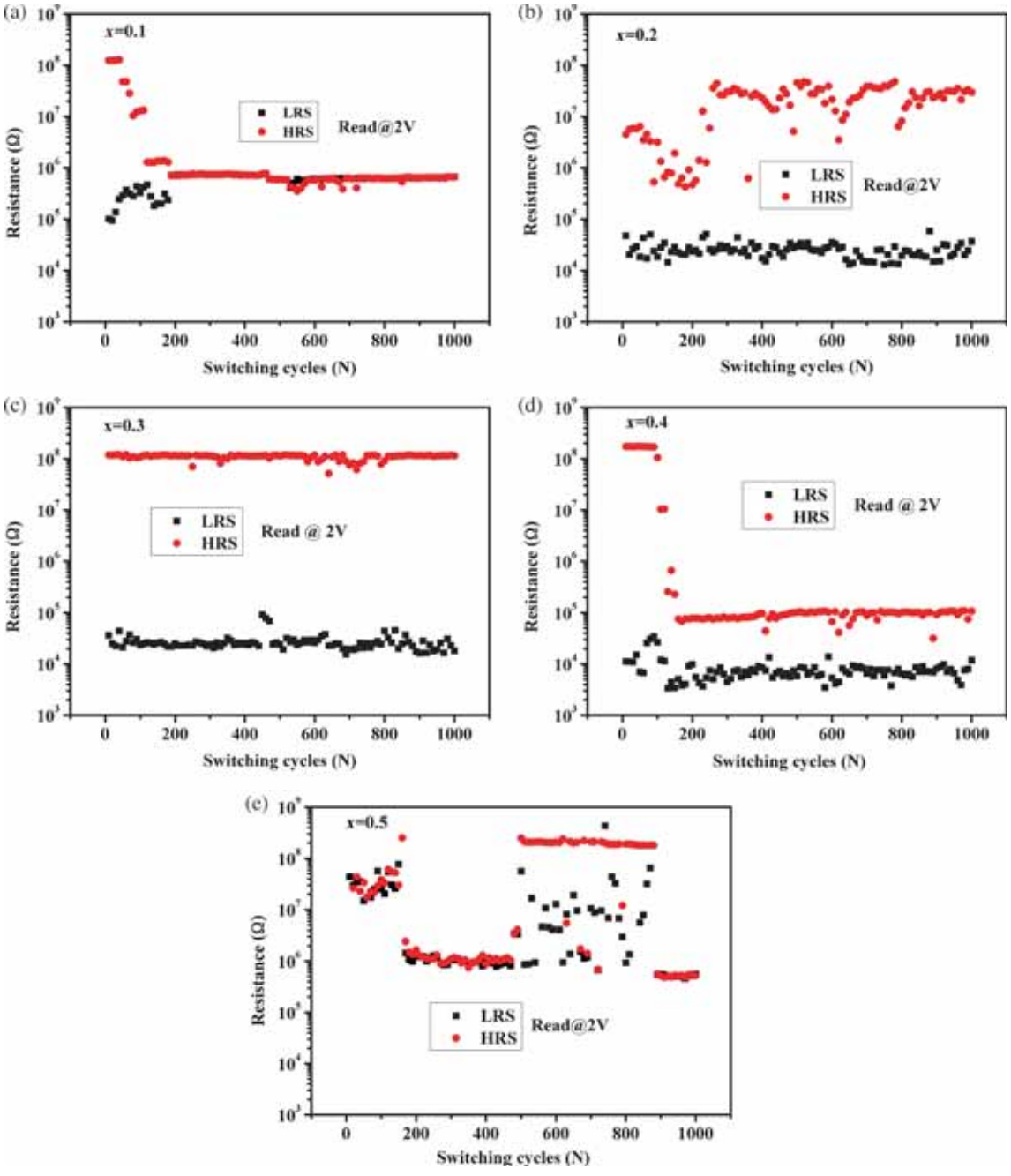

Figure 5. The reading endurance and stability of the $Ag/La_{1-x}Zn_xMnO_3/p^+$-Si devices.

increases within the films. Under the voltage bias, the trapping of defects near the interfaces may form a space charge region. When the space charge region becomes sufficiently large, the dominant conduction mechanism gradually changes from Schottky emission to SCLC. When the opposite bias is applied, for $x = 0.1$, the conducting filaments rupture and then the mechanism changes back to the Schottky emission. For $x \geq 0.2$, the space charge region decreases, and then the SCLC conduction changes back to the Schottky emission.

Figure 5 shows the repeatable RS behaviour of the $Ag/La_{1-x}Zn_xMnO_3/p^+$-Si memory devices. The figure shows the evolution of R_{HRS} and R_{LRS} in 1000 cycles under a reading voltage of 2 V every 10 cycles. The endurance performances of the $Ag/La_{1-x}Zn_xMnO_3/p^+$-Si devices are different. For $x = 0.1$, the R_{HRS}/R_{LRS} ratio is larger than 10^3 in the beginning, and then gradually decreases and finally disappears. For $x = 0.2$, the device still exhibited RS characteristics after 1000 repeated sweep cycles; however, the R_{HRS}/R_{LRS} ratio has a larger range of 10^2–10^4. For $x = 0.3$, the R_{HRS}/R_{LRS} ratio of the device has no obvious degradation during 1000 I–V cycles, i.e., $>10^3$. For $x = 0.4$, the R_{HRS}/R_{LRS} ratio of the device is more than 10^3 in the beginning, gradually decreases, and then finally remains stable at 10. For $x = 0.5$, the resistance does not change in the beginning. After about 500 cycles, it starts to change but shows disorder, and finally disappears again. As can be seen from figure 5, the device with $x = 0.3$ has the best read/write endurance characteristics, in which it shows steady and reproducible bipolar RS behaviour after 1000 switching cycles. A previous study showed that the conductive mechanism of the $Re_{1-x}A_xMnO_3$ system may be the electrons jumping in Mn^{4+}–O–Mn^{3+}; in addition, the defect density and Mn^{4+}/Mn^{3+} ratio change accordingly with the increase of the amount of doped Zn in the films [20], resulting in different endurance performances. Studies have shown that the RS characteristics of the $La_{1-x}A_xMnO_3$ with $x \approx 0.3$ have better properties [9–11,20,21].

The fluctuating scope of set voltage (V_{set}) and reset voltage (V_{reset}) is an important feature of RRAM, which can reflect the stability and applicability of a device. The cumulative probabilities of the V_{set} and V_{reset} of $Ag/La_{1-x}Zn_xMnO_3/p^+$-Si during 1000 RS cycles with different Zn concentrations are shown in figure 6. Only the cycles for $x = 0.2$, 0.3 and 0.4 are presented because the devices with $x = 0.1$ and 0.5 exhibited poor fatigue properties. As shown in figure 6, V_{set} and V_{reset} are distinguishable under the bipolar mode. With change in concentration of doped Zn, the V_{set} and V_{reset} exhibited small differences; the V_{set} ranges from 2.5 to 5 V with centre of 4 V, and the V_{reset} ranges from −2.5 to −5 V with centre of −4 V.

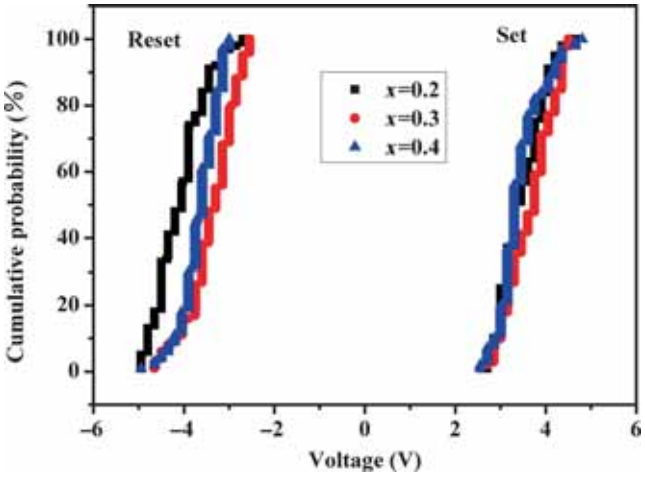

Figure 6. The cumulative probabilities of the set and reset voltages of $Ag/La_{1-x}Zn_xMnO_3/p^+$-Si during the 1000 resistive switching cycles.

4. Conclusion

$La_{1-x}Zn_xMnO_3$ ($x = 0.1$, 0.2, 0.3, 0.4, 0.5) thin films fabricated using the sol–gel method on p^+-Si substrate are amorphous after annealing at 600°C for 1 h in ambient air. The $Ag/La_{1-x}Zn_xMnO_3/p^+$-Si devices exhibited excellent bipolar resistance characteristics. The statistic distribution of V_{set} and V_{reset} is significantly tight and distinguishable. The endurance characteristics of the device are different. The device with $x = 0.3$ shows the best read/write endurance characteristics as well as steady and reproducible bipolar RS behaviour after 1000 switching cycles. The R_{HRS}/R_{LRS} ratio is more than 10^3. The results of current fitting showed that the dominant conduction mechanism of the $Ag/La_{1-x}Zn_xMnO_3/p^+$-Si devices can be explained by the Schottky emission mode in HRS. However, the dominant conduction mechanism varies in LRS with the change in Zn doping concentration. At $x = 0.1$, the dominant mechanism is filamentary conduction, whereas at $x \geq 0.2$, the dominant mechanism is SCLC conduction.

Acknowledgements

This work has been financially supported by the Natural Science Foundation of China (project no. 51262003) and Guangxi Key Laboratory of Information Materials (Guilin University of Electronic Technology), China (project no. 1110908-10-Z).

References

[1] Sawa A 2008 *Mater. Today* **11** 28

[2] Torrezan A C, Strachan J P, Medeiros Ribeiro G and Williams R S 2011 *Nanotechnology* **11** 485203

[3] Liu S Q, Wu N J and Ignatiev A 2000 *Appl. Phys. Lett.* **76** 2749

[4] Yan Z B, Guo Y Y, Zhang G Q and Liu J M 2011 *Adv. Mater.* **23** 1351

[5] Chang W Y, Lai Y C, Wu T B, Wang S F, Chen F T and Tsai M J 2008 *Appl. Phys. Lett.* **92** 022110

[6] Hu P, Li X Y, Lu J Q, Yang M, Lv Q B and Li S W 2011 *Phys. Lett. A* **375** 1898

[7] Waser R, Dittmann R, Staikov G and Szot K 2009 *Adv. Mater.* **21** 2632

[8] Potember R S, Pochler T O and Cowan D O 1979 *Appl. Phys. Lett.* **34** 405

[9] Musarrat H, Dong R, Choi H J, Lee D S, Seong D J, Pyun M B and Hwang H 2008 *Appl. Phys. Lett.* **92** 202102

[10] Yang R, Li X M, Yu W D, Liu X J, Gao X D, Wang Q and Chen L D 2009 *Appl. Phys. A* **97** 85

[11] Bhavsara K H, Joshia U S, Mistry B V, Khan S A and Avasthi D K 2011 *Radiat. Eff. Defect. Solids* **166** 718

[12] Liu L M, Liu J and Jin Y J 2010 *J. Chin. Ceram. Soc.* **38** 1876

[13] Shima H, Zhong N and Akinaga H 2009 *Appl. Phys. Lett.* **94** 082905

[14] Choi B J, Jeong D S, Kim S K, Rohde C, Choi S, Oh J H *et al* 2005 *J. Appl. Phys.* **98** 033715

[15] Jameson J R, Fukuzumi Y, Wang Z, Griffin P, Tsunoda K, Meijer G I and Nishi Y 2007 *Appl. Phys. Lett.* **91** 112101

[16] Yang Y C, Pan F, Liu Q, Liu M and Zeng F 2009 *Nano Lett.* **9** 1636

[17] Liu Q, Guan W H, Long S B, Jia R, Liu M and Chen J N 2008 *Appl. Phys. Lett.* **92** 012117

[18] Luo J M, Lin S P, Zheng Y and Wang B 2012 *Appl. Phys. Lett.* **101** 062902

[19] Li S, Wei X H and Zeng H Z 2013 *Appl. Phys. Lett.* **103** 133505

[20] Liu D Q, Wang N N, Wang G, Shao Z Z, Zhu X, Zhang C Y and Cheng H F 2013 *Appl. Phys. Lett.* **103** 134105

[21] Liu X J, Li X M, Wang Q, Yu W D, Yang R, Cao X *et al* 2010 *Solid State Commun.* **150** 137